LPDynR: a new tool to calculate the Land Productivity Dynamics indicator

Xavier Rotllan-Puig[1], Eva Ivits[2], and Michael Cherlet[3, ✉]

[1] ASTER Projects. Barri Reboll, 9, 1r. 08694 Guardiola de Berguedà (Barcelona), SPAIN

[2] European Environment Agency. Geospatial Information Services Group. Copenhagen, DENMARK

[3] European Commission – Joint Research Centre (JRC). Directorate D – Sustainable Resources. Unit D6 – Knowledge for Sustainable Development & Food Security Unit. Via Enrico Fermi 2749. I-21027 Ispra (VA), ITALY

✉ Correspondence: Michael Cherlet <michael.cherlet@ec.europa.eu>

Keywords: Land Productivity, Ecosystem Dynamics, Land Degradation, Desertification, Vegetation

Abstract

As part of the UN Sustainable Development Goal 15 (Life on Land), the indicator 15.3.1 is adopted to measure the Land Degradation Neutrality. Land Degradation Neutrality is addressed as stable —or increasing— state in the amount and quality of land resources required to support ecosystem functions and services and enhance food security during a certain period of time. It is a binary indicator (i.e. degraded/not degraded), expressed as the proportion of land that is degraded over total land area within each land type, and is based on three sub-indicators: (1) Trends in Land Cover, (2) Land Productivity and (3) Carbon Stocks.

The Land Productivity sub-indicator (LP) refers to the total above-ground Net Primary Production and reflects changes in health and productive capacity of the land. Declining trends interpreted with ancillary data such as e.g. information on non-adapted agricultural practices possibly combined with low income can be usually understood as land degradation. LP can be calculated using the Land Productivity Dynamics (LPD) approach, which is the methodological basis of the R-based tool *LPDynR* presented in this article. It uses vegetation-related indices (phenology and productivity) derived from time series of remote sensed vegetation indices to estimate ecosystem dynamics and change. The final result of the LPD indicator is a categorical map with 5 classes of land productivity dynamics, ranging from declining to increasing productivity. As an example of *LPDynR* functionalities, we present a case study for Europe.

1 Introduction

The United Nations General Assembly designed in 2015 a collection of 17 global goals, so called Sustainable Development Goals (SDGs; UN, 2015), with the general aim of "achieving a better and more sustainable future for all", and which are intended to be accomplished by 2030. Each SDG is subdivided into a list of targets which, in turn, go together with indicators to be able to measure their progress and success. Such indicators have to be credible, based on standardized methodologies and, often, have to be spatially explicit (Dubovyk, 2017).

The SDG-15, entitled Life on Land, has among its targets the 15.3, which expects "to combat desertification, restore degraded land and soil, including land affected by desertification, drought and floods, and strive to achieve a land degradation-neutral world". In this context, Land Degradation Neutrality (LDN) is defined as the stable (or increasing) state regarding the amount and quality of land resources required to support ecosystem functions and services and enhance food security during a certain period of time (UNCCD, 2015).

The indicator 15.3.1 is adopted to measure the LDN and is expressed as the proportion of land that is degraded over total land area. It is a binary indicator (i.e. degraded/not degraded) based on three sub-indicators calculated separately: (1) Trends in Land Cover, (2) Land Productivity and (3) Carbon Stocks (Sims et al., 2020, 2017). While the first two can capture relatively fast changes, carbon stocks reflect slower changes which suggest a longer-term trajectory (Orr et al., 2017). Following a "one-out-all-out" process, the indicator identifies an area as degraded if one of the sub-indicators shows

degradation. The three sub-indicators must be comparable among territories and based on standardized sources and methods. The data can be collected through existing sources, such as maps, reports or databases, but also can be derived from Earth observation (EO) imagery using remote sensing tools.

The Land Productivity sub-indicator (LP), addressed in this document, approximates the total above-ground net primary productivity (NPP), which can be defined as the total energy fixed by plants minus their respiration. Such energy is transformed into biomass which, in turn, allows ecosystems to develop their functions and deliver essential services. Therefore, LP reflects changes in health and productive capacity of the land and its declining trends can be usually understood as land degradation (Cherlet et al., 2018; Prince, 2009; Yengoh et al., 2015). The World Atlas of Desertification (Cherlet et al., 2018) suggests that the LP sub-indicator can be calculated using the Land Productivity Dynamics (LPD) approach. LPD was first developed by Ivits and Cherlet (2013) and is the methodological basis of the *LPDynR* tool presented in this article.

2 Land Productivity Dynamics and *LPDynR*

The Land Productivity Dynamics (LPD) approach is based fundamentally on the use of time series of vegetation-related indices derived from remote sensed imagery, such as the normalized difference vegetation index (NDVI) or the plant phenology index (PPI). NDVI, for example, can be used as a proxy for land productivity, as many studies at global and local scales have identified a strong relationship between NDVI and NPP (Ivits and Cherlet, 2013; Prince, 2009; Yengoh et al., 2015, and references therein). The LPD approach often uses phenological and productivity-related variables derived from

time series of NDVI, given that these can provide additional information on several aspects of vegetation/land cover functional composition in relation to ecosystem dynamics and change (E. Ivits, M. Cherlet, Mehl, et al., 2013). These dynamics of the ecosystems, which might eventually drive land degradation, can be caused by human activities and/or biophysical processes, as well as other processes indirectly tied to them, such as climate change (Yengoh et al., 2015). While the most commonly used phenological parameters are the beginning and the end date of the vegetation growing season, together with the season length in number of days, the ones related to land productivity are e.g. accumulations of vegetation index values over time, mostly during the growing season as defined by the season start and end date. These approximate NPP within the growing season.

The final result of the LPD indicator is a categorical map with 5 classes of land productivity dynamics, ranging from declining to increasing productivity over a target time period. It is the result of a combined assessment of two sources of information, as seen in Figure 1. The first layer is the Long-Term Change Map. In general terms, it shows the tendency of change of land productivity (positive or negative) and the effect on productivity levels that this tendency might have had on a particular original point after a certain period of time. The second layer is the Current Status Map, which provides information on the current levels of land productivity in relation to its potential, being current the end of the target time period. It compares the local productivity with the range of productivity across similar areas in terms of land cover or bioclimatic traits (Sims et al., 2017). Further explanations for both branches will be given in the respective sections below.

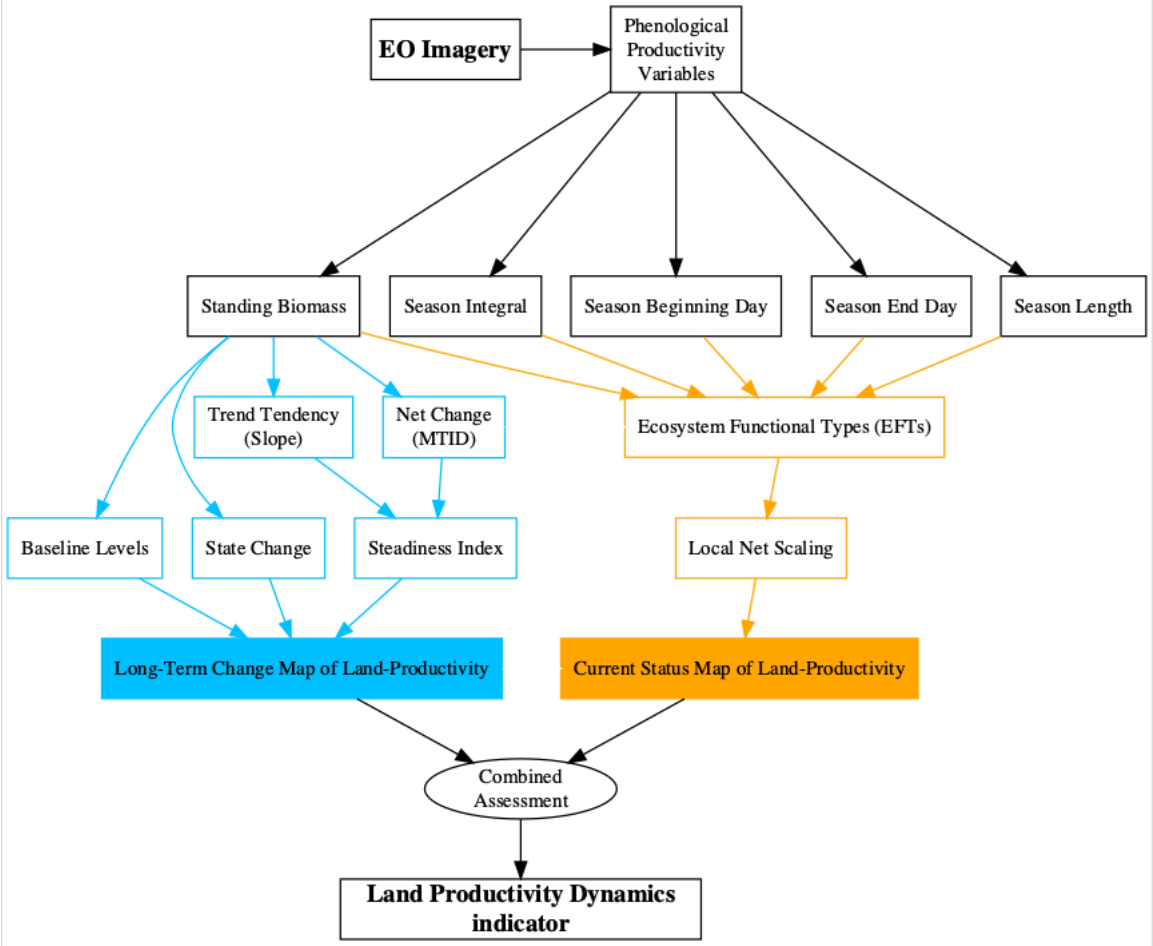

Figure 1: Flowchart of the process to calculate the Land Productivity Dynamics indicator and used by LPDynR

Following the LPD approach, *LPDynR* is an R-based tool (i.e. an R package) which allows the user to produce the final Land Productivity Dynamics Map using as inputs a set of time series of phenological and/or productivity variables (multi-band GeoTIFF rasters). By means of the different functions included in the package, it produces intermediate layers (e.g. Steadiness Index, Ecosystem Functional Types; see Figure 1) which are used to calculate both the Long-Term Change Map and the Current Status Map. In addition, several parameters can be set along the process in order to reflect the

117 preferences of the user. The functions included in the package have no limitations
118 regarding the number of years included in the time series, the variables to use or the
119 spatial extent and resolution. While *LPDynR* v1.0.1 can be installed from CRAN
120 (https://CRAN.R-project.org/package=LPDynR), the latest version is available at
121 https://github.com/xavi-rp/LPDynR.

122 3 Data set preparation

123 A case study is presented in order to illustrate the methodology implemented in the
124 *LPDynR* package to calculate the LPD indicator. In this case, a data set of 5 phenological
125 and productivity-related variables were used, at European level and on a 0.5km of spatial
126 resolution, produced by the European Environment Agency - European Commission
127 (EEA). They are all derived from time series (2000-2019) of MODIS imagery and its
128 derived product Plant Phenology Index (PPI; Jin and Eklundh, 2014). PPI is linearly
129 related to the canopy green leaf area index (LAI) and has a temporal pattern very similar
130 to the one shown by the gross primary productivity (GPP) estimated by flux towers at
131 ground reference stations. The five variables are produced using the software TIMESAT
132 (Jönsson and Eklundh, 2004). At the moment of writing this article, these time series are
133 not yet published, however more information about the previous freely distributed data
134 set (2000-2016) by the EEA can be found in their website
135 (https://sdi.eea.europa.eu/catalogue/srv/eng/catalog.search#/home). For example, the
136 details for above ground vegetation productivity can be found in
137 https://sdi.eea.europa.eu/catalogue/srv/eng/catalog.search#/metadata/29ae2d47-7af2-
138 4c09-ba5f-e2fbb7c2b0d1. The five variables used were:

- Above ground vegetation productivity (from now on, SB)
- Above ground season vegetation productivity (from now on, CF)
- Start of vegetation growing season (from now on, SBD)
- End of vegetation growing season (from now on, SED)
- Vegetation growing season length (from now on, SL)

In the *LPDynR* v.1.0.1, the functions use multi-band GeoTIFF rasters to start the process, one per phenological/productivity variable. Each band of each raster contains one of the years of the time series.

It is also important to note that *LPDynR* comes with a sample data set, which can be used to run tests, as well as some examples in the form of "vignettes" attached to the package.

4 Long Term Change Map of land productivity

As seen in Figure 1 and explained above, the Land Productivity Dynamics indicator is produced by combining two input layers. The first layer is the Long-Term Change Map (also called "tendency map"). The tendency layer combines information on the trend of land productivity dynamics (positive or negative), the level of productivity of the ecosystem at the start of the time series, as well as whether it has changed its productivity state or not in the period under study (Ivits and Cherlet, 2013). Using such multi-source information for the Long-Term Change Map instead of a trend significance assessment was chosen to better describe the state and change of ecosystems. For instance, even though vegetation development presents a long-term negative dynamics (e.g. negative slope of a linear trend), the negative trend might not be strong enough to decrease the

level of productivity such that the starting productivity state changes drastically. This could result to be a non-significant trend in linear trend analysis leaving the pixel out for further analysis which is not wishful in the land degradation analysis. The way in which the three sources of information are calculated for the Long Term Change Map using a land productivity variable is described in the following subsections.

4.1 Steadiness Index

The first of the three metrics which integrates the Long-Term Change Map represents the long-term tendency of change of the natural systems, being either positive or negative. This metrics is the Steadiness Index (Ivits, Cherlet, Sommer, et al., 2013) and can be calculated using the function *steadiness()*. The Steadiness Index is based on the combination of two other metrics which are calculated per pixel by the same function: (1) the slope derived from fitting a linear trend on the time series and (2) the net change of the productivity level of the same period.

The use of a linear regression would imply to respect the linear trend results by strict statistical assumptions for confidence intervals and significance tests, such as heteroscedasticity, normal distribution of the errors, no autocorrelation between the observations and a deterministic process. Most often, these assumptions are not accomplished when working with time series of remote sensed products, and the use of non-parametric trend measures are not adequate either (Ivits, Cherlet, Sommer, et al., 2013). This is why the Steadiness Index only keeps classes of tendency and no more tests are run for assessing its significance. Therefore, only the sign (positive or negative) of the slope of the trend is kept as the value of each pixel's tendency of ecosystem dynamics. In

addition, the net change of the productivity variable, in the units of the applied vegetation index, is calculated for the same time window and per pixel using the Multi-Temporal Image Differencing method (MTID; Guo et al., 2008). Afterwards, MTID is also transformed into positive or negative net change. Finally, the two classes of both metrics (slope of the linear function and net change category) are combined into four "steadiness" categories as seen in Table 1. Figure 2A represents the 4-class map of the Steadiness Index for the case study.

Table 1: Description of the four Steadiness Index classes and how they are derived based on the combination of the signs of both the slope of the linear function and the net change

Steadiness Class	Slope	Net Change	Description
Steadiness1	-	-	Strong negative ecosystem dynamics (possibility changing equilibrium)
Steadiness2	-	+	Moderate negative ecosystem dynamics (likely remain in current equilibrium)
Steadiness3	+	-	Moderate positive ecosystem dynamics (likely remain in current equilibrium)
Steadiness4	+	+	Strong positive ecosystem dynamics (possibility changing equilibrium)

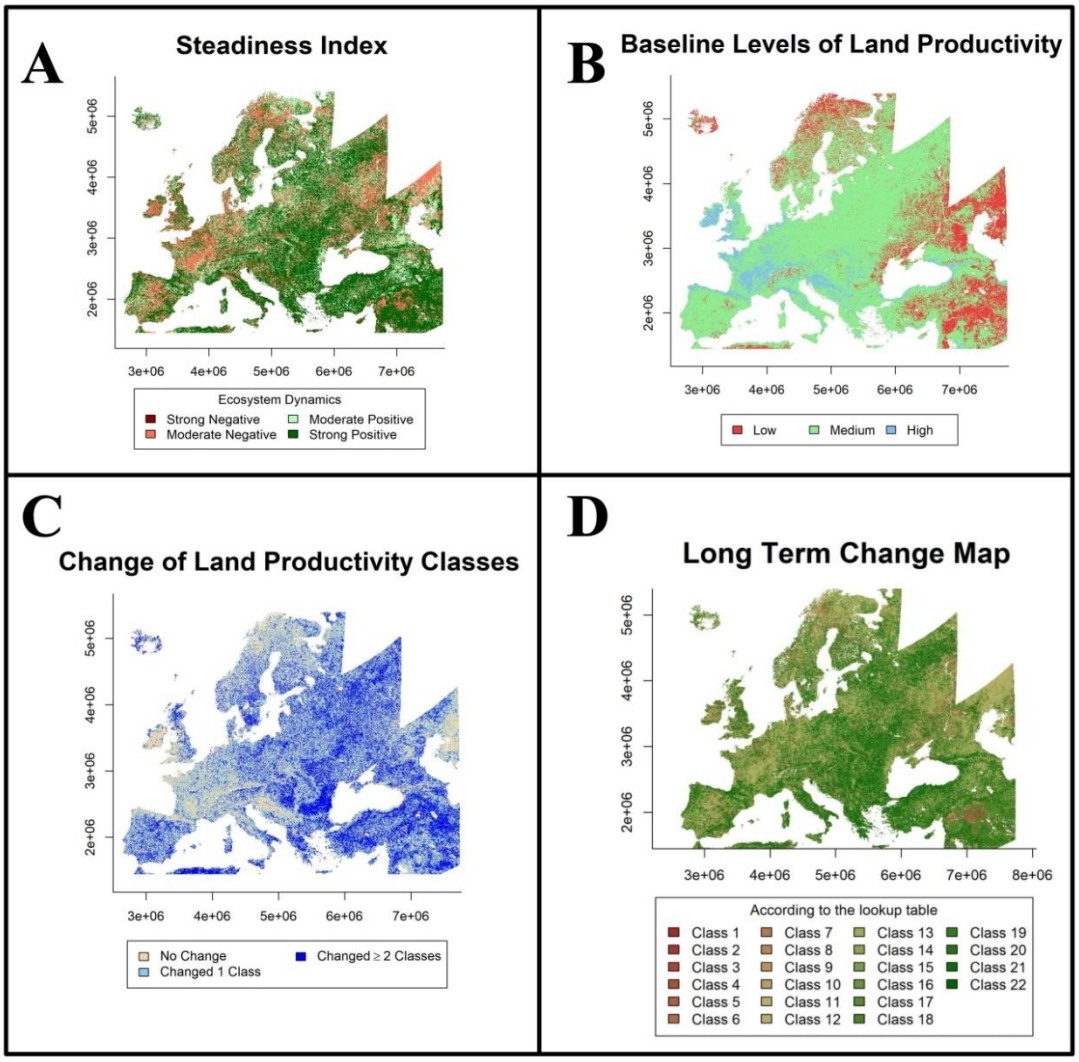

192

193 *Figure 2: (A) Steadiness Index, (B) baseline levels and (C) state change maps for the case study*
194 *based on the 'Above ground vegetation productivity' variable. (D) Land productivity Long Term*
195 *Change Map for the case study based on the combination of the previous three maps.*
196 *Descriptions respectively in sections 4.1, 4.2, 4.3 and 4.4*

197

4.2 Baseline levels of productivity

The second source of information for the derivation of the Long-Term Change Map is the baseline levels of the productivity variable at the beginning of the time series.

For the calculation of the baseline levels of land productivity at the beginning of the time series, *LPDynR* categorizes productivity values into three classes: low, medium and high. To do that, the function *baseline_lev()* averages the first *n* years of the time series in order to avoid extreme events, such as abnormal droughts in wet areas, etc, which would skew the distribution of productivity values into too high or low values. The number of years to be considered by the average function can be set by passing the argument *yearsBaseline* to the function. The default value is 3 years; averaging more years would move the baseline value closer to the mean of the time series, which would not describe the baseline anymore.

After the average of the *n* number of years is calculated, *baseline_lev()* first classifies the pixels into 10 classes using 10-quantiles equalling to the corresponding percentile levels. The reason for this intermediate step is that, if directly opted for three classes (i.e. low, medium and high), the number of pixels per category would be classified homogeneously (i.e. 33.3% of pixels/class), which is a statistically correct but an over simplified representation of baseline status. Instead, *LPDynR* allows the user to define the percentile level to be used based on local knowledge. For example in dryland ecosystems or in boreal regions different average productivity level can be defined as low, medium or high values. The United Nations Development Programme (UNPD, https://www.undp.org) for example declares that 40% of the World's land resources are drylands (Middleton et al.,

2011), while the World Atlas of Desertification updated this proportion to 37.2% (Cherlet et al., 2018). Therefore, in global applications one might choose 37.2% of pixels to be classified as "low level" of productivity. Consequently, as default, the global application of *LPDynR* classifies the first four groups of pixels, i.e. 40 percentile (after rounding 37.2%), as "low" baseline productivity level, the five consecutive groups between 50 and 90 percentile as "medium" productivity level and the rest 10% of pixels with the highest average productivity levels, as "high" baseline. Both the proportion of pixels classified as low level and high level of land productivity can be set by passing to *baseline_lev()* the arguments *drylandProp* and *highprodProp*, respectively. The function classifies the rest of the pixels ((100 - (*drylandProp* + *highprodProp*)) as medium level. The assumption of classifying 40% of pixels as low productive is valid at global level, however, the proportion of drylands/low level of productivity should be modified for local and regional studies. For example, at the European level, drylands cover 20% of total land (FAO, 2019). This proportion has been used in the case study and the resulting 3-class map showing the estimation of levels of productivity at the beginning of the time series can be seen in Figure 2B.

4.3 Change of state of productivity

The third layer used for the land productivity Long-Term Change Map is the change of the state of the productivity level during the time window under study. This aspect is necessary for land degradation assessments as it reports whether pre-set productivity state thresholds have been surpassed or not, which can be a consequence of either the natural

241 resilience, new land use/practices that have been introduced, or impacts of other
242 manmade or natural phenomena (Ivits and Cherlet, 2013).

243 To calculate the state change per pixel, the function *state_change()* uses both the
244 productivity baseline level at the beginning of the time series, as described in the
245 previous subsection, and the productivity state level at the end of the time series. This
246 final state is calculated in the same way as the baseline level, i.e. (1) averaging the last 3
247 years and (2) classifying into 10 categories using 10-quantiles. The reason for using a 10-
248 class classification is that it would be difficult to approximate if the change of one state to
249 another was due to a big or a small change. Instead, using the 10-class classification for
250 the final productivity state, one can address if a pixel has moved from class 5 to 4 (small
251 change) or from class 9 to 4 (big change).

252 Once the class change per pixel has been calculated, either with positive or negative
253 results, the map is categorized into 3 final classes: (1) no change, (2) changed between 1
254 and *x* classes or (3) changed more than *x* classes, where *x* can be defined by the user by
255 passing the argument *changeNclass* to the function (default is 1). See Figure 2C for a
256 map of the state change in the case study.

257 4.4 Long Term Change Map

258 The land productivity Long-Term Change Map is one of the two pillars of the LPD
259 indicator (Figure 1) calculated with *LPDynR*. This map is calculated by the combination
260 of the Steadiness Index, the productivity levels at the beginning of the time series and the
261 change of the state of productivity between the beginning and the end of the time series.

The function *LongTermChange()* performs the combination of the three qualitative metrics mentioned before into the Long-Term Change Map, resulting in 22 new categories as shown in Table 2. The resulting map for the case study is presented in Figure 2D.

Table 2: Lookup table for the land productivity Long Term Change Map (Steadiness Index + BaseLine Levels + State Change)

	Change of productivity at the end of the time series		
Steadiness Index / Baseline productivity	**No Change**	**Changed 1 to *x* classes**	**Changed > *x* classes**
St1 low	1	2	3
St1 med.	4	5	6
St1 high	7	8	9
St2 low	10	10	10
St2 med.	11	11	11
St2 high	12	12	12
St3 low	13	13	13
St3 med.	14	14	14
St3 high	15	15	15
St4 low	16	17	18
St4 med.	19	20	21
St4 high	22	22	22

At this point, the user might want to finalise the LPD calculation avoiding the second part of the methodology proposed by Ivits and Cherlet (2013), which is the Current Status Map of Land Productivity. To do this, the function *LPD_CombAssess* (see further explanations in the respective subsection below) can be called to reclassify the 22-class Long-Term Change Map into the final 5 classes of LPD.

5 Current Status Map of land productivity

The Land Productivity Dynamics indicator is composed of two base layers: the Long-Term Change Map of Land Productivity and the Current Status Map of Land Productivity (as shown in Figure 1). After the long-term productivity dynamics described previously (i.e. Long-Term Change Map) is calculated, the second source of information needed is the current level of land productivity. For this purpose, a Local Net Scaling approach is implemented (Prince, 2009). Such approach estimates the level of land productivity of each pixel relative to its neighbours with similar characteristics of their land functions. In other words, it calculates the potential level of productivity of each pixel within a homogeneous land unit. The Current Status Map may help, for instance, to identify areas which, although having a positive trend of productivity over time, their levels of current productivity are low relative to the pixels in the same homogeneous land unit and, thus, they might be still suffering land degradation (Sims et al., 2017). A first step for the calculation of the Current Status Map, therefore, is the derivation of the homogeneous land units across the area of study.

5.1 Ecosystem Functional Types (EFTs)

The methodology implemented in *LPDynR* to derive homogeneous land units, or Ecosystem Functional Types (EFTs), is adapted from Ivits, Cherlet, Horion et al. (2013). It is basically a clustering process which uses, in this case, phenological and productivity variables to create the ecosystem functional groups. Among the different unsupervised clustering techniques available for data grouping, K-means has been chosen. K-means is

296 widely used in data science mainly due to its relative simplicity of implementation and
297 interpretation.

298 Originally, the unsupervised classification was performed after a three-steps pre-
299 processing of the phenology and productivity variables (see Chapter 3, Dataset
300 preparation): (1) removing highly correlated variables to avoid multicollinearity; (2) a
301 first Principal Component Analysis (PCA) to select the optimal number of PCs and their
302 associated variables showing the highest loadings; and (3) a final PCA to clearly
303 associate each PC with one variable. However, test runs in this study (see Supplementary
304 Material S1) have shown that the final LPD indicator does not differ significantly when it
305 is derived using the raw phenological/productivity variables. Therefore, although the two-
306 PCAs step is also implemented in *LPDynR*, only the removing of highly correlated
307 variables (e.g. $|r| > 0.7$) is recommended before running the k-means clustering.

308 In order to check for multicollinearity among the variables, the function *rm_multicol()*
309 first calculates their averages among the years of the time series. Then, the process
310 internally runs the function *removeCollinearity()* from the package *virtualspecies* (Leroy
311 et al., 2016). This function allows the user to set up the minimum Pearson's correlation
312 absolute value, which can be modified by passing the argument *multicol_cutoff*. It is
313 established to be $r = 0.7$ as default. A subset of random points of the data set can be used
314 for the calculation of the correlation coefficient in case the rasters have a large number of
315 pixels and the user wants to speed up the process. The default number of randomly
316 selected points is 10% of total pixels in the raster. However, the number of points can be
317 selected by passing *sample.points = FALSE* and *nb.points* equal to the required amount
318 of points. Finally, the function automatically creates a multi band raster where each band

319 corresponds to one randomly selected variable of each group of correlation. In addition, a
320 dendrogram to visualize the groups of intercorrelated variables can be plotted if the user
321 wants to, although not by default. For the present case study, which was run with five
322 variables, the dendrogram produced can be seen in Supplementary Material S2. At the
323 cut-off value of r = 0.7, three groups of intercorrelated variables were found and one
324 variable of each group was selected to continue with the analysis (i.e. CF, SED and SL).

325 In case the user would like to run the two-PCAs steps, both the first "screening PCA",
326 which is done over the uncorrelated variables, and the "final PCA" are subsequently
327 performed with the same function *PCAs4clust()*. In order to know the optimal number of
328 variables to be used in the "final PCA", a threshold of cumulative variance of the PCs is
329 implemented. This threshold is established to be 0.9, i.e. 90% of the variance of the
330 variables explained, as default.

331 Finally, the clustering algorithm can be run over either the selected PCs or the
332 uncorrelated raw (phenology and productivity) variables using the function *EFT_clust()*.
333 This function uses *kmeans()* from the package *stats*. K-means is an iterative unsupervised
334 method, one of the main limitations being that it is not able to optimize the number of
335 clusters by itself. Instead, the optimal number of clusters needs to be determined by the
336 user. In the *LPDynR* package, the optimal number of clusters can be determined using the
337 "scree-plot method". This method is implemented with the function *clust_optim()* and it
338 is based on running several K-means clustering with different number of clusters each, in
339 order to assess how the quality of the models change with the number of clusters. Then, a
340 plot is produced with the number of clusters in the x-axis and the total within-cluster sum
341 of squares in the y-axis. A break line, the so-called "elbow", indicates the number of

clusters where the quality of the model no longer improves substantially as the number of clusters (model complexity) increases. In the present study the clustering was run with ten different number of clusters (5 to 50, with the increment of 5) to give a good amount of points to plot the curve, and the maximum number of iterations was set to 10 (see the plot produced in Supplementary Material Figure S3.1).

The "scree plot" method undoubtedly has some level of subjectivity, as the user decides where the curve flattens enough for the appropriate number of clusters. Alternatively, to remove such subjectivity, several numerical methods exist to calculate the optimal number of clusters, although they take also some statistical assumptions. These methods might be explored in the future if a higher level of accuracy is believed to be necessary or if the process shall be performed without user intervention. In addition, other hierarchical clustering methods could be explored in order to avoid calculating the optimal number of clusters beforehand, although previous tests run with ISODATA have been shown to be highly resource demanding, especially in terms of computing time.

Once the optimal number of clusters is estimated, the final clustering is run with the function *EFT_clust()* using the defined number of clusters and passed with the argument *n_clust*. Other parameters which can be passed to the function *EFT_clust()* are those that will be passed to *stats::kmeans()*, such as *nstart*, *iter.max* or *algorithm* (see https://stat.ethz.ch/R-manual/R-devel/library/stats/html/kmeans.html for further information). It is important to note that when setting the argument *nstart*, the larger the value the more accurate the clustering result will be. This is because the function uses different sets of starting random centroids and runs the clustering *nstart* times. From these number of clustering runs, the best classification result is chosen. Therefore, a

365 larger *nstart* value increases the chances of having a better cluster classification. In
366 addition, *kmeans()* can use different algorithms to perform the clustering (e.g.
367 "MacQueen", "Hartigan-Wong", etc.; see references in *kmeans()* documentation). As
368 stated in the function documentation (*?kmeans*), "Hartigan-Wong" usually gives better
369 results, although it is recommended to try several starts (*nstart > 1*). However, when
370 using "Hartigan-Wong" with a (too) large number of clusters, and a lot of values of the
371 variables are very similar, *kmeans()* is not able to converge in an acceptable amount of
372 time (even increasing the number of iterations with *iter.max*). In these cases when the
373 clustering does not converge, instead of stopping the process with an error, the function
374 *kmeans()* only gives a warning after finishing the clustering, so that the obtained clusters
375 are based on a non-converged process. Diminishing the number of clusters or rounding
376 variables' values might be good strategies to help *kmeans()* to converge.

377 *EFT_clust()* produces a RasterLayer object, where each pixel is linked to a cluster, plus
378 an index of the clustering performance, which measures the compactness of individuals
379 (i.e. pixels) within the groups. This index, which is expected to be as high as possible, is
380 calculated as:

381 $$CI = \frac{BSS}{TSS} \times 100 \quad (1)$$

382 where *CI* is the compactness index, *BSS* is between-cluster sum of squares (i.e.
383 *betweenss*, provided by *kmeans()*) and *TSS* is total sum of squares (i.e. *totss*, also
384 provided by *kmeans()*).

385

Finally, as previous tests of K-means with up to 100 iterations were showing problems to converge in a certain limit of time, the maximum number of iterations is set to 500 as default in the function. Within this number of iterations and rounding variables, for almost all the tests performed, the process did achieve convergence with no issues (see Supplementary Material S4). For the running example, the EFTs resulted from the whole process can be seen in Figure 3A.

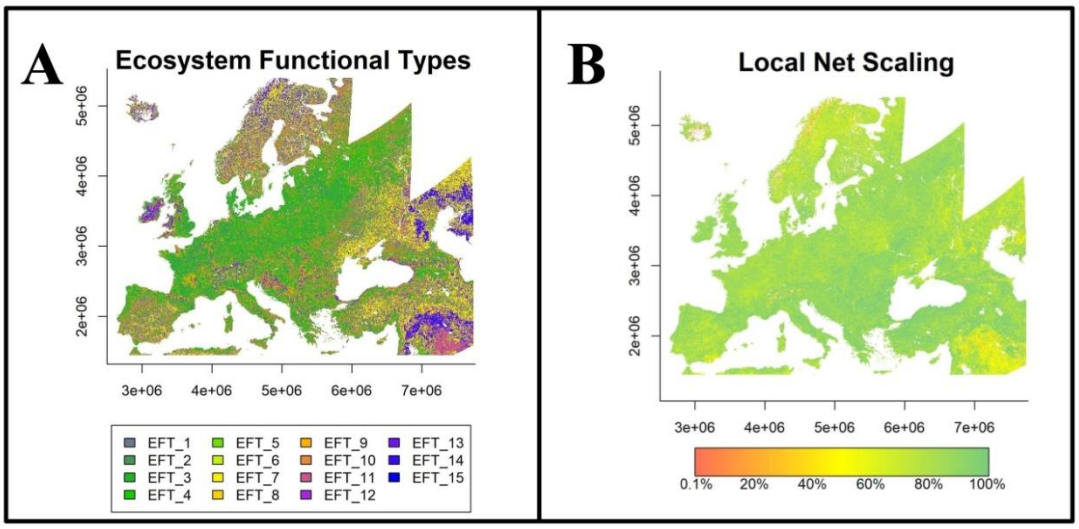

Figure 3: (A) Ecosystem Functional Types (EFTs) derived from phenological and productivity variables using the K-means clustering method. (B) Local Net Primary Production Scaling (LNS): proportion of annual production (i.e. average of the last 5 years of cyclic fraction) over the local potential production (i.e. the 90-percentile within the Ecosystem Functional Type)

5.2 Local Net Production Scaling

The Local Net Primary Productivity Scaling (from now on, Local Net Scaling or LNS) method (Prince, 2009) is based on the use of multi-temporal satellite data to calculate the difference between the potential and actual NPP for each pixel in homogeneous land

401 functional units. Potential productivity in the *LPDynR* method is defined as the
402 productivity level which could be reached without human influence in natural landscapes
403 (Prince, 2009, and references therein) or as the result of human activity e.g. in agriculture
404 areas or managed forests, and is estimated as the maximum value of productivity within
405 each EFT. The deviation of the productivity found in a particular place and time as
406 referred to the local maximum within its phenological homogeneous cluster, reflects a
407 level of productivity anomaly which is useful for the productivity status map (Ivits and
408 Cherlet, 2013).

409 The cyclic fraction of vegetation productivity (e.g. the summed NDVI over the growing
410 season) is widely used as a proxy for the estimation of the current land productivity
411 (Fensholt, 2013), as it incorporates both natural and anthropogenic factors which define
412 the inter-annual variability of land production. Therefore, it represents that part of the
413 standing biomass which is potentially appropriated to be used by humans and the
414 environment (Ivits and Cherlet, 2013) and it is the one appropriated to calculate the LNS.

415 The function *LNScaling()* is implemented in *LPDynR* to calculate the LNS. The
416 productivity variable (i.e. CF) and the EFTs clusters as explained under 5.1 are passed to
417 *LNScaling()* to calculate the potential productivity within each EFT. Instead of the
418 maximum productivity value within each cluster, the 90-percentile value is established as
419 the potential productivity value, given that values higher than this threshold could be
420 outliers. Finally, the LNS for each pixel is calculated as

421 $$LNS = \frac{AP}{PP_{EFT}} \quad (2)$$

where *AP* is the annual production of the pixel (i.e. the average of the last 5 years of cyclic fraction) and PP_{EFT} is the potential production within its EFT (i.e. the 90-percentile).

For the calculation of the final LPD indicator (i.e. combined assessment), the Local Net Scaling values are aggregated into two categories: (1) LNS pixels with less than 50% of the potential local production (within the EFT) and (2) LNS pixels with more or equal to 50% of potential local production. This percentage, being 50% the default in *LPDynR*, can be set by the user.

The result for the LNS calculation is presented in Figure 3B.

6 Combined assessment of land productivity

The Land Productivity Dynamics indicator, as shown in the processing flowchart in Figure 1, is based on the combination of two main sources of information: a map of the tendency, positive or negative, of the level of land productivity along the time series, and another map capturing the current level of productivity of each pixel relative to the maximum productivity in a homogeneous land area. As seen above, both branches to calculate the indicator are qualitative methods. Therefore, the final LPD indicator, produced with the function *LPD_CombAssess()*, is also a qualitative measure with 5 possible values or categories after the reclassification of each pixel as shown in Table 3. Such categories are (1) d - Declining, (2) ed - Early signs of decline, (3) st - Stable but stressed, (4) sn - Stable and not stressed and (5) i - Increasing land productivity.

Table 3: Lookup table for the combination of the two branches assessment (i.e. Long Term Change Map and Current Status Map of land productivity) to derive the Land Productivity Dynamics categories (i.e. (1) d - Declining land productivity, (2) ed - Early signs of decline of land productivity, (3) st - Stable but stressed land productivity, (4) sn - Stable and not stressed land productivity and (5) i - Increasing land productivity). The Local Scaling is defined as 50% by default, but it can be modified by the user

Steadiness I.	**Baseline L.**	**State Change**	**Local Scaling**	
			< 50%	**>= 50%**
st1	lo	0	d	ed
st1	lo	1	d	ed
st1	lo	2	d	d
st1	me	0	d	ed
st1	me	1	d	ed
st1	me	2	d	d
st1	hi	0	ed	st
st1	hi	1	d	ed
st1	hi	2	d	ed
st2	lo	0	st	st
st2	me	0	st	st
st2	hi	0	st	st
st3	lo	0	sn	sn
st3	me	0	sn	sn
st3	hi	0	sn	sn
st4	lo	0	sn	i
st4	lo	1	sn	i
st4	lo	2	i	i
st4	me	0	sn	i
st4	me	1	i	i
st4	me	2	i	i
st4	hi	0	i	i

In the present study, the Land Productivity Dynamics indicator final map (Figure 4) is the result of the combined assessment of the Long Term Change Map (Figure 2D) and the Current Status Map of land productivity (Figure 3B), both based on the "Above ground

vegetation productivity" variable, plus the two phenological variables for the derivation of the EFTs.

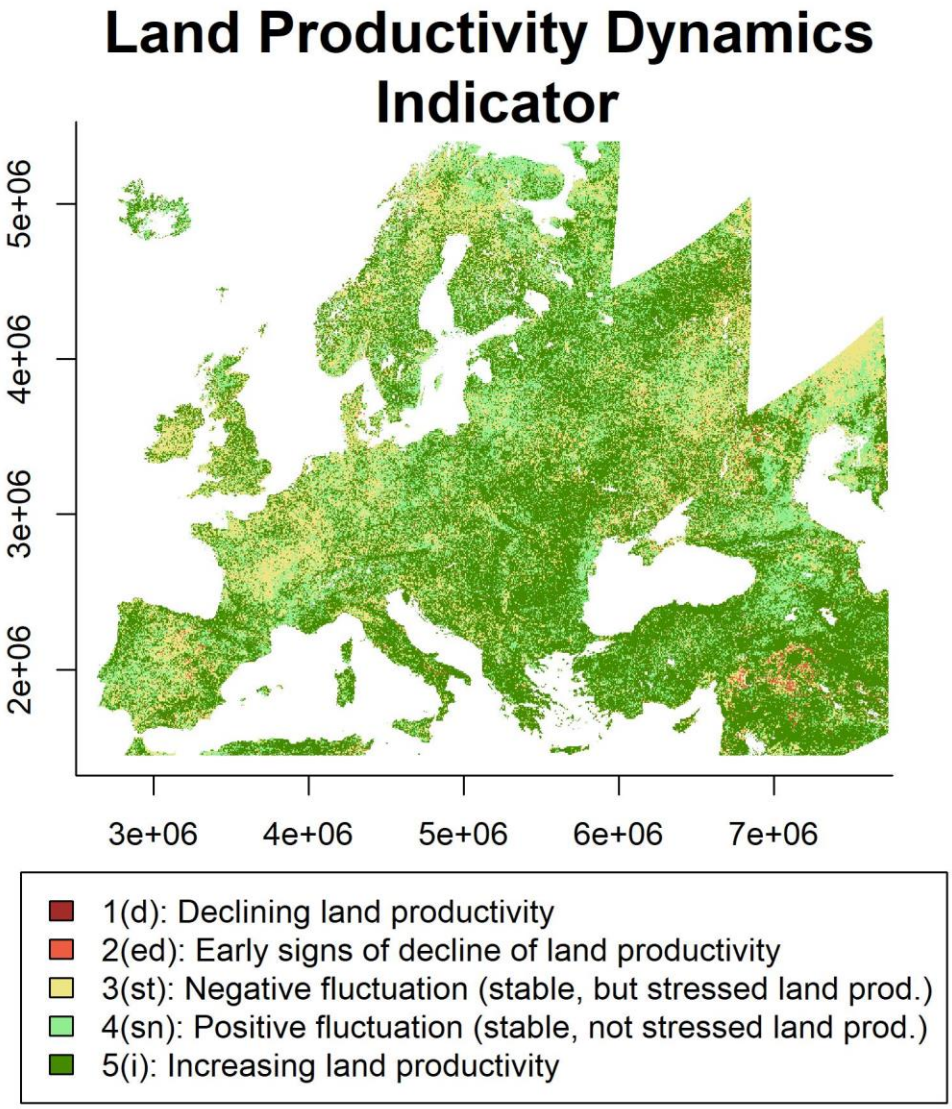

Figure 4: Land Productivity Dynamics indicator final map. Combined assessment of the Long Term Change Map and the Current Status Map of land productivity.(1) d - Declining land productivity, (2) ed - Early signs of decline of land productivity, (3) st - Stable but stressed land productivity, (4) sn - Stable and not stressed land productivity and (5) i - Increasing land productivity

6.1 Alternative method for the Land Productivity Dynamics indicator

Including the current level of land productivity relative to its potential (Chapter 5) in the final LPD calculation (Chapter 6) improves the land productivity indicator as LNS values may indicate not degradation in areas with a negative tendency of productivity, but where the level of productivity still remains high relative to other similar areas nearby. Despite this, the user might want to derive the final product based only on the tendency map (i.e. Long Term Change Map; Chapter 4), avoiding the inclusion of the Current Status Map derived with the Local Net Scaling approach. The function *LPD_CombAssess()* performs this step by passing the argument *LandProd_current = NULL*. By doing so, the function reclassifies the Long Term Change Map into the same 5 categories of the LPD indicator described above. Table 4 shows how the function executes the reclassification.

Table 4: Lookup table for the reclassification of the Long Term Change Map into the Land Productivity Dynamics categories (i.e. (1) d - Declining land productivity, (2) ed - Early signs of decline of land productivity, (3) st - Stable but stressed land productivity, (4) sn - Stable and not stressed land productivity and (5) i - Increasing land productivity)

Steadiness I.	Baseline L.	State Change	LPD class
st1	lo	0	d
st1	lo	1	d
st1	lo	2	d
st1	me	0	d
st1	me	1	d
st1	me	2	d
st1	hi	0	ed
st1	hi	1	d
st1	hi	2	d
st2	lo	0	st
st2	me	0	st
st2	hi	0	st
st3	lo	0	sn
st3	me	0	sn
st3	hi	0	sn
st4	lo	0	sn
st4	lo	1	sn
st4	lo	2	i
st4	me	0	sn
st4	me	1	i
st4	me	2	i
st4	hi	0	i

A comparison of the final LPD indicator map produced using the combined assessment (i.e. Long Term Change Map + Current Status Map) with the one developed without the Current Status Map can be seen in Figure 5 (Map 1 and Map 2, respectively). In addition, the "differences map" in the same figure represents pixels which have a different class between the two approaches. The difference between the classes was always equal to

491 minus 1, indicating that the difference between the two approaches is only one class.
492 Furthermore, the combined indicator using the LNS approach had higher values in all
493 cases indicating a better potential to differentiate between land productivity conditions.
494 Table 5 shows the number of pixels which changed from one class to another. From this
495 table it can be seen how pixels never changed from negative to positive dynamics (class 3
496 to 4) or from positive to negative (class 4 to 3).

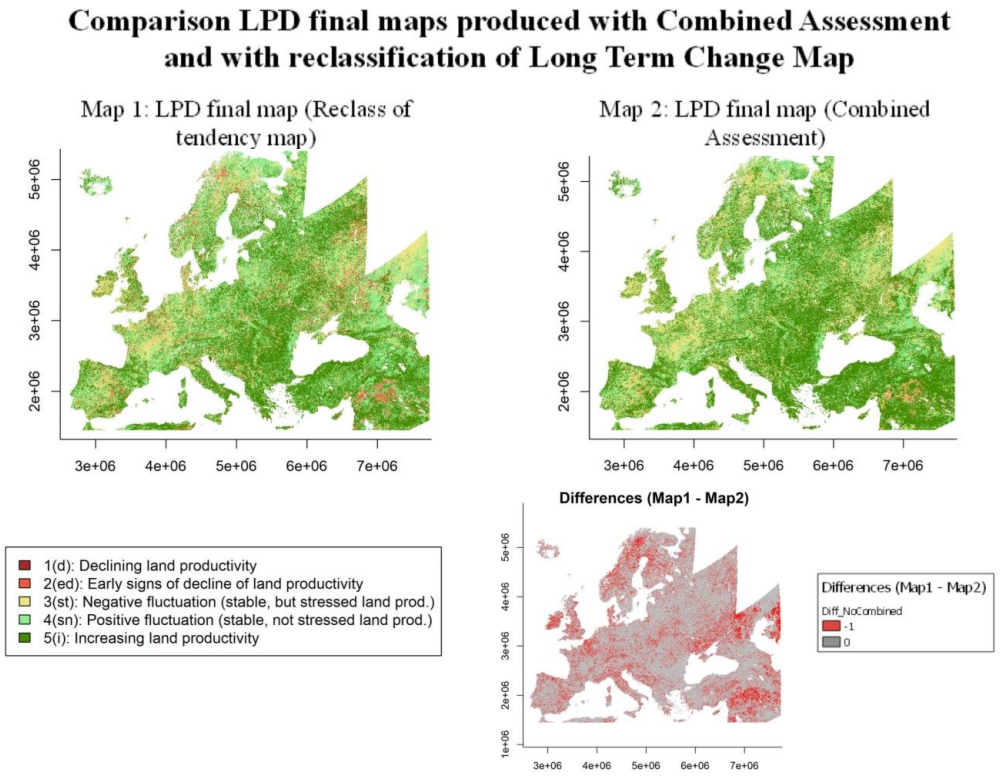

497

498 *Figure 5: Land Productivity Dynamics indicator final maps derived by the reclassification of the*
499 *Long Term Change Map of land productivity (Map 1) and produced by the combined assessment*
500 *(Map 2; Long Term Change Map + Current Status Map). Differences Map (Map 1 - Map2)*
501 *represents in red those pixels showing different resulting classes from both approaches*

502

Table 5: Number of pixels showing different class in the combined assessment approach and in the non-combined one (i.e. reclassification of the Long Term Change Map). Only these three combinations were found in the case study

Non-combined Assessment - Class	Combined Assessment - Class	Number Pixels	Description
1	2	2439370	Declining to early signs of decline
2	3	355412	Early signs of decline to Stable but stressed
4	5	4964183	Stable not stressed to Increasing

Finally, Figure 6 shows the proportion of pixels per LPD class under each approach, both for the whole extent (i.e. Europe) and also splitting the map by biogeographical regions. The biogeographical regions were defined with the official delineations used in the Habitats Directive (92/43/EEC) and for the EMERALD Network, which are freely distributed as a spatial data set by the European Environmental Agency - European Commission (https://www.eea.europa.eu/data-and-maps/figures/biogeographical-and-marine-regions-in).

The plots show that there were some differences in the proportion of pixels per class for each of the two approaches. For example, the Alpine, the Anatolian, and the Steppic regions were the three showing more differences, which ranged from 12.1 to 15.5% for some LPD classes. This fact evidences the added value of including the Current Status Map in the calculations to refine the LPD indicator final results.

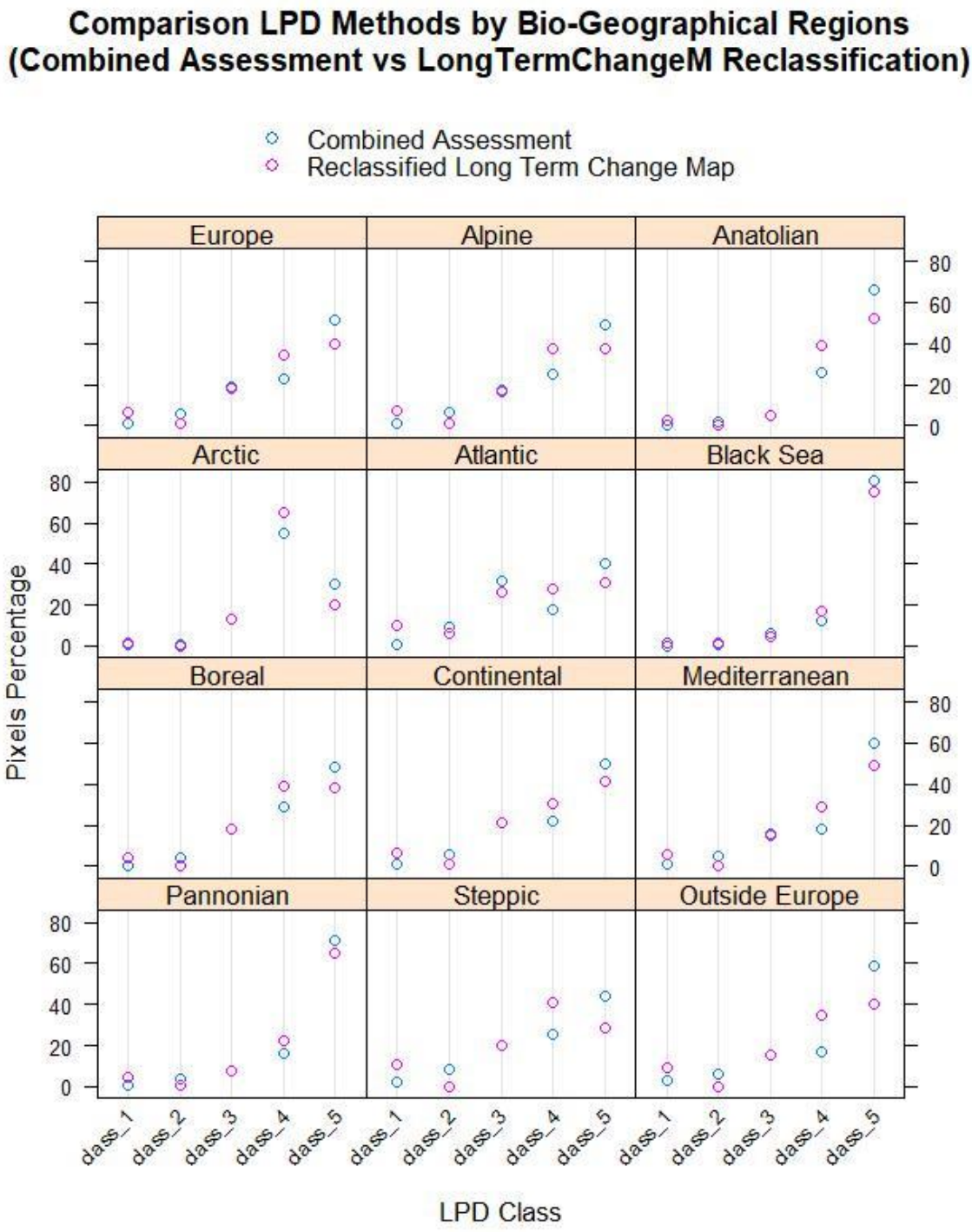

520

521 *Figure 6: Proportion of pixels per LPD class for the combined assessment (light blue) and for the*
522 *reclassified Long Term Change Map (purple), for Europe and by biogeographical regions*

523

6.2 Land Productivity Dynamics partial indicator

As seen in the previous subsections regarding the derivation of the tendency map (i.e. Long Term Change Map; Chapter 4), the final result is related to the extremes of the time series. In case the time series is long, the LPD indicator shows a long term assessment of what has happened regarding the land productivity dynamics between the beginning and the end of the period in the study. However, to understand the dynamics of the biomass within the observation period, as well as to assess the stability of the final product, it might be useful to produce several "partial LPD indicators" using different time windows of the time series.

This process is not yet implemented in *LPDynR* as a function, but we propose the following code to produce partial LPD maps of *n* years and with an overlap of *y* years between the end of the last period and the beginning of the next one. This example was implemented for the same case study shown along this article and the final partial LPD maps can be seen in Figure 7.

```
## Running LPDynR for partial time series ##

ts_length <- 5                                  # time series length to run 'partial LPD maps'
ts_years_overlap <- 2                           # number of years of overlapping
partial_dir <- "/LPD_partial"                   # directory to save the 'partial LPD' results
first_year <- 1                                 # first year of the whole time series
last_year <- nlayers(cf)                        # last year of the whole time series
last_year_run <- first_year + ts_length - 1     # last year of the 'partial LPD'

while(last_year_run <= last_year){
  # subsetting the years (layers) to run
  cf_run <- cf[[first_year:last_year_run]]

  # a directory to save the data
  dir2save0 <- paste0(getwd(), partial_dir)
  if(!dir.exists(dir2save0)) dir.create(dir2save0)
  dir2save <- paste0(getwd(), partial_dir, "/LPD_", first_year, "_", last_year_run, "/")
  if(!dir.exists(dir2save)) dir.create(dir2save)

  ##                                      ##
  ##                                      ##
  ## Here all the steps to calculate the  ##
  ## final LPD map as in the examples     ##
  ##                                      ##
  ##                                      ##

  # Cleaning temp
  removeTmpFiles(h = 0.5)

  # Parameters for the loop
  first_year <- last_year_run - ts_years_overlap + 1
  last_year_run <- first_year + ts_length - 1
}
```

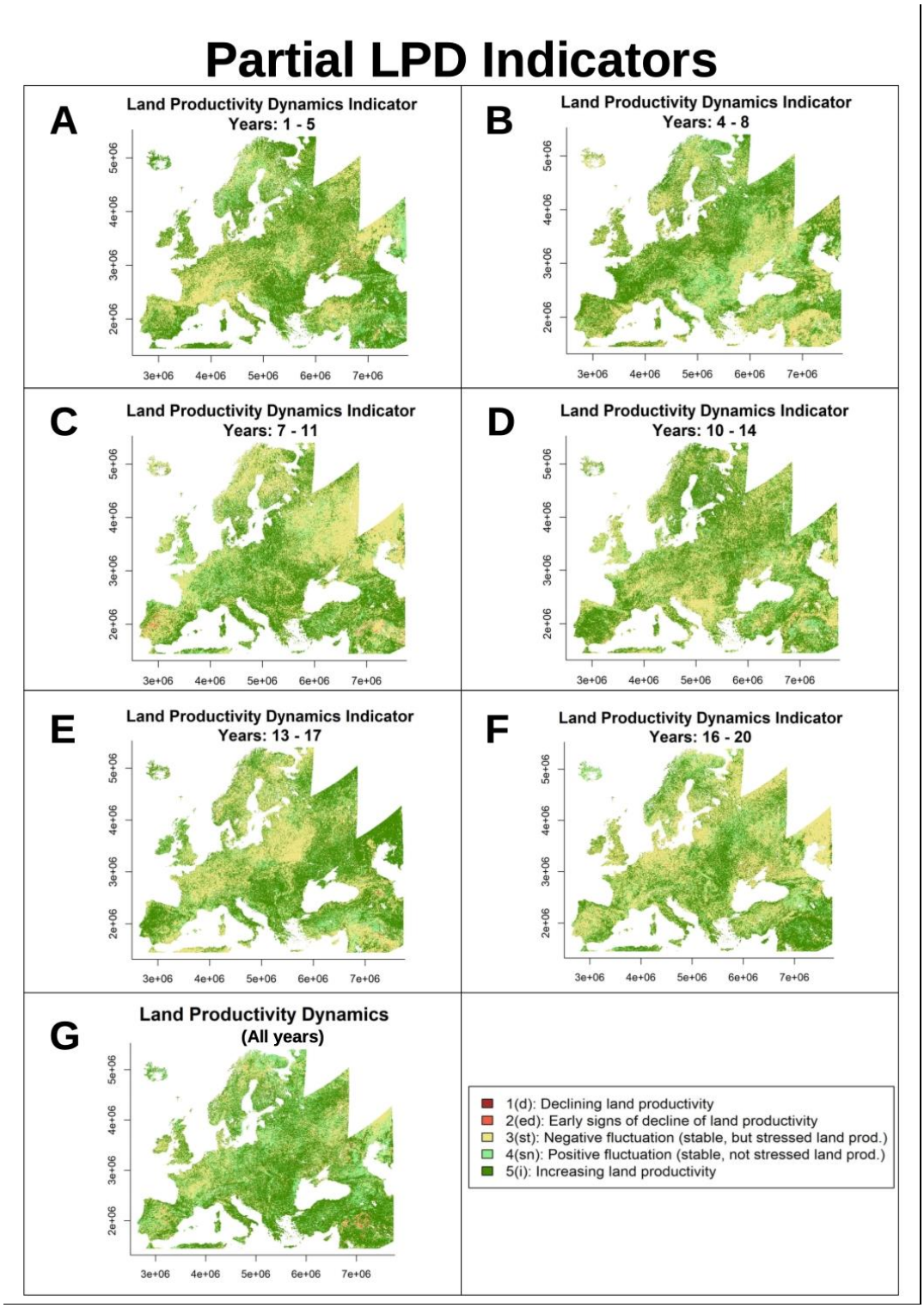

Figure 7: Partial LPD indicators (plots A to F) and LPD indicator for the whole time series (plot G). The partial LPD indicators were produced for time windows of 5 years with an overlap of 2 year between the end of the last period and the beginning of the next one

The complete LPD indicator (i.e. for the whole time series; Figure 7G) shows, in general terms, a positive trend pattern across Europe (i.e. more pixels in greens). However, some of the intermediate plots show more negative trends (i.e. yellow and light red pixels). This, besides demonstrating the highly fluctuating character of vegetation, confirms the influence of the extremes of the time series on the final result. In this sense, in the time series of the example, the first period seemed to show stressed vegetation in terms of productivity for most of the pixels in Western/Central Europe, and they expressed a large increase around years 7/8. Such increase caused a large number of areas belonging to the higher LPD class, and it still influenced the dynamics of the following period, resulting in areas with stressed vegetation.

The fact that the LPD indicator calculated with the approach included in *LPDynR* is influenced by the beginning and the end of the time series is not a limitation, as the main goal of the LPD indicator is to know the current state of vegetation in relation to a previous state, and not the fluctuations due to, for example, to extreme climatic events such as e.g. droughts. However, being able to map these fluctuations in space and time might add information for further analysis.

7 Conclusions

As stated by the Intergovernmental Science-Policy Platform on Biodiversity and Ecosystem Services (IPBES), land degradation leads to a loss of biodiversity and a reduction of ecosystem functions and delivered services all over the world. Therefore, combating land degradation and restoring degraded lands has become an urgent priority in order to protect all life on Earth as well as to ensure human well-being (IPBES, 2018).

In this sense, satellite observations provide valuable data which might help to monitor the Earth's land cover to evaluate the state of land degradation.

The Land Productivity Dynamics indicator (LPD), as part of the SDG-15.3.1 indicator, aims at contributing to the assessment of the state of land degradation and desertification at global, regional and local scales. Therefore, the *LPDynR* new tool has been developed to derive the LPD indicator using phenological and land productivity variables, which can be obtained from long-term time series of Earth observation imagery.

LPDynR is a comprehensive set of open source programming code, written in the well-known R language and properly packaged, ready to be freely distributed in order to let the users with a minimum knowledge of the R language calculate the LPD indicator. The package, once installed, includes several examples and a small data set for testing the functionalities and the different parameters to tune them.

8 References

Cherlet, M., Hutchinson, C., Reynolds, J., Hill, J., Sommer, S., Maltitz, G. von (Eds.), 2018. World atlas of desertification. Publication Office of the European Union, Luxembourg.

622 Dubovyk, O., 2017. The role of remote sensing in land degradation assessments:
623 Opportunities and challenges. European Journal of Remote Sensing 50, 601–613.
624 https://doi.org/10.1080/22797254.2017.1378926

625 FAO, 2019. Trees, forests and land use in drylands: The first global assessment (FAO
626 Forestry Paper No. 184). FAO, Rome.

627 Fensholt, K.K., Rasmus Rasmussen, 2013. Assessing land degradation/recovery in the
628 african sahel from long-term earth observation based primary productivity and
629 precipitation relationships. REMOTE SENSING 5, 664–686.

630 Guo, W.Q., Yang, T.B., Dai, J.G., Shi, L., Lu, Z.Y., 2008. Vegetation cover changes and
631 their relationship to climate variation in the source region of the yellow river, china,
632 1990–2000. International Journal of Remote Sensing 29, 2085–2103.
633 https://doi.org/10.1080/01431160701395229

634 IPBES, 2018. The ipbes assessment report on land degradation and restoration.
635 Montanarella, l., scholes, r., and brainich, a. (Eds.). Secretariat of the
636 Intergovernmental Science-Policy Platform on Biodiversity; Ecosystem Services,
637 Bonn, Germany.

638 Ivits, E., Cherlet, M., 2013. Land-productivity dynamics towards integrated assessment
639 of land degradation at global scales (Technical Report No. EUR 26052). Joint
640 Research Centre of the European Commission.

641 Ivits, E., Cherlet, M., Horion, S., Fensholt, R., 2013. Global biogeographical pattern of
642 ecosystem functional types derived from earth observation data. Remote Sensing 5,
643 3305–3330. https://doi.org/10.3390/rs5073305

644 Ivits, E., Cherlet, M., Mehl, W., Sommer, S., 2013. Ecosystem functional units
645 characterized by satellite observed phenology and productivity gradients: A case
646 study for europe. Ecological Indicators 27, 17–28.
647 https://doi.org/10.1016/j.ecolind.2012.11.010

648 Ivits, E., Cherlet, M., Sommer, S., Mehl, W., 2013. Addressing the complexity in non-
649 linear evolution of vegetation phenological change with time-series of remote
650 sensing images. Ecological Indicators 26, 49–60.
651 https://doi.org/https://doi.org/10.1016/j.ecolind.2012.10.012

652 Jin, H., Eklundh, L., 2014. A physically based vegetation index for improved monitoring
653 of plant phenology. Remote Sensing of Environment 152, 512–525.
654 https://doi.org/https://doi.org/10.1016/j.rse.2014.07.010

655 Jönsson, P., Eklundh, L., 2004. TIMESAT—a program for analyzing time-series of
656 satellite sensor data. Computers & Geosciences 30, 833–845.

657 Leroy B., Meynard C.N., Bellard C., Courchamp F., 2016. virtualspecies, an R package
658 to generate virtual species distributions. Ecography 39, 599-607.
659 https://doi.org/10.1111/ecog.01388

660 Middleton, N., Stringer, L., Goudie, A., Thomas, D., 2011. The forgotten billion. MDG
661 achievement in the drylands. United Nations Development Programme, New York,
662 NY, 10017, USA.

663 Orr, B.J., Cowie, A.L., Castillo Sanchez, V.M., Chasek, P., Crossman, N.D., Erlewein,
664 A., Louwagie, G., Maron, M., Metternicht, G.I., Minelli, S., Tengberg, W., A. E.,

Welton, S., 2017. Scientific conceptual framework for land degradation neutrality. In: A report of the science-policy interface. UNCCD, Bonn, Germany.

Prince, I.R., S. D. Becker-Reshef, 2009. Detection and mapping of long-term land degradation using local net production scaling: Application to zimbabwe. REMOTE SENSING OF ENVIRONMENT 113, 1046–1057.

Sims, N.C., Barger, N.N., Metternicht, G.I., England, J.R., 2020. A land degradation interpretation matrix for reporting on un sdg indicator 15.3.1 and land degradation neutrality. Environmental Science & Policy 114, 1–6. https://doi.org/https://doi.org/10.1016/j.envsci.2020.07.015

Sims, N.C., Green, C., Newnham, G.J., England, J.R., Held, A., Wulder, M.A., al., 2017. Good practice guidance sdg indicator 15.3.1. Proportion of land that is degraded over total land area, First. ed. United Nations Convention to Combat Desertification.

UN, 2015. Transforming our world: The 2030 agenda for sustainable development (No. A/RES/70/1). United Nations.

UNCCD, 2015. Integration of the sustainable development goals and targets into the implementation of the United Nations convention to combat desertification and the report of the intergovernmental working group on land degradation neutrality (No. ICCD/COP(12)/4). UNCCD Conference of the Parties, Ankara, Turkey.

Yengoh, G.T., Dent, D., Olsson, L., Tengberg, A.E., Tucker, C.J., 2015. Use of the normalized difference vegetation index (ndvi) to assess land degradation at multiple scales, Springer briefs in environmental science. Springer.